Structural Engineering and Mechanics, *Vol. 74, No. 3 (2020) 445-455*
DOI: https://doi.org/10.12989/sem.2020.74.3.445

Investigation of shear lag effect on tension members fillet-welded connections consisting of single and double channel sections

Moien Barkhori[1a], Shervin Maleki[2b], Masoud Mirtaheri*[3], Meissam Nazeryan[2c] and S.Mahdi S.Kolbadi[3d]

[1]Department of Civil Engineering, University of Jiroft, Jiroft, Iran
[2]Department of Civil Engineering, Sharif University of Technology, Tehran, Iran
[3]Department of Civil Engineering, K.N. Toosi University of Technology, Tehran, Iran

(Received February 23, 2020, Revised March 12, 2020, Accepted March 27, 2020)

Abstract. Shear lag phenomenon has long been taken into consideration in various structural codes; however, the AISC provisions have not proposed any specific equation to calculate the shear lag ratio in some cases such as fillet-welded connections of front-to-front double channel sections. Moreover, those equations and formulas proposed by structural codes are based on the studies that were conducted on riveted and bolted connections, and can be applied to single channel sections whilst using them for fillet-welded double channels would be extremely conservative due to the symmetrical shape and the fact that bending moments will not develop in the gusset plate, resulting in less stress concentration. Numerical models are used in the present study to focus on parametric investigation of the shear lag effect on fillet-welded tension connection of double channel section to a gusset plate. The connection length, the eccentricity of axial load, the free length and the thickness of gusset plate are considered as the key factors in this study. The results are then compared to the estimates driven from the AISC-LRFD provisions and alternative equations are proposed.

Keywords: shear lag; tension members; net section fracture; double channel section

1. Introduction

In order to design tension members, various fracture modes including tensile yielding in the gross section, tensile rupture in the net section, shear yielding or rupture of the element, and block shear rupture must be taken into account. This study focuses on the second fracture mode, in which the tensile rupture occurs in the section adjacent to the connection. The main reason of fracture in a gross section is that not all of the sectional area contributes in transferring the tensile load to the gusset plate, and as such, stress concentration would develop in the section adjacent to the connection, making it a potential fracture point. The described phenomena is called shear lag and is parametrically investigated for single or double channel (front-to-front) sections in the present study.

Regarding that early studies on tension members particularly started in the mid-twentieth century, those previous researches related to the context of this study will be briefly presented as follows. Munse and Chesson (1963) conducted an experimental research on riveted and bolted joints to determine the effective factors in strength reduction of a tension member. Numerous experiments were performed on different members including single plates, single channels, double channels either connected to one side or both sides of the gusset, I-shaped built up members, single and double channels. To design tension members, the authors finally proposed several equations which were subsequently used by other researchers as well as structural code committees (Easterling and Gonzalez Giroux, 1993). The research by Benaddi D. and Bauer D. (2003) investigated the ultimate tensile and compressive strength of single channels and apparently revealed that the outer fibers of the sections yield and therefore, the load influence line and the eccentricity of load are shifted. Based on these observations, a new equation was introduced to calculate the net section area.

Gaylord *et al.* (1992) tried to calculate the net section area and derived a practical equation consisting of four separate factors, one of which was the shear lag coefficient acquired. Easterling *et al.* (1993) studied the shear lag effect on fillet-welded connections by a number of experiments. They used 27 experimental specimens including plates, hot-rolled channels and channels while the channels were connected to the gusset plate in a back-to-back form. The results revealed that shear lag significantly affects the tensile strength of plates and channels; however, channel sections do not experience much of a reduction in the tensile strength. Meanwhile, the upper bound of 0.9 for shear lag coefficient is set to cover the effects of eccentricity as well as other constructional defects. Wang Qf (1997) investigate about lateral buckling of thin-walled members with openings considering shear lag using numerical analysis.

Oribison *et al.* (1998) conducted experiments on the

*Corresponding author, Associate Professor
E-mail: mmirtaheri@kntu.ac.ir
[a] Research Associate
E-mail: moien.barkhori@gmail.com
[b] Professor
E-mail: smaleki@sharif.edu
[c] M.Sc.
E-mail: m94nazeryan@gmail.com
[d] Ph.D. Student
E-mail: Mahdi_kolbadi@sina.kntu.ac.ir

http://www.techno-press.com/journals/sem&subpage=7
ISSN: 1225-4568 (Print), 1598-6217 (Online)

connections of WT-shape and single channel members, considering the fracture modes as follows: block shear rupture, net section tensile rupture, and gross section tensile yielding. According to those experiments, the AISC-LRFD provisions are averagely conservative to be used for WT-shape sections whereas the results provided by the code equations for single channels are a bit non-conservative. In addition, no extensive yielding along the shear plane were seen during the described experiments and it was only around the bolts that local yielding occurred. Luigino Dezi et al. (2003) presented a model for demonstrating the shear lag effect in twin girder composite deck. Later, Humphries *et al.* (2004) examined and compared the performance of fillet-welded connections of various tension members such as plates, single or double channels (connected in a variety of possible forms), HSS (Hollow Structural Section) and channel sections. The study illustrated that structural code provisions are actually conservative in many cases and need to be revised in order to achieve a more economical design. Besides, it was concluded that double channel sections performed better than built-up box sections in terms of tensile strength. Also, Won-Sup Hwang *et al.* (2004) evaluated the shear lag parameters for beam-to-column connections in steel piers. In their study, the evaluation method for shear lag stresses has been investigated by comparing analytical stresses with test results.

L. H. Teh and V. Yazici (2013) examined the “three factors” approach via double channels having no connection eccentricity. According to the result of this study, the test results affirm the three factors approach, and it was found that the back-to-back channel braces were affected by local bending even though the connection eccentricity was nominally zero. Lip H. The *et al.* (2013) investigated the Net Section Tension Capacity of Cold-Reduced Sheet Steel Channel Braces Bolted at the Web through considering three distinct factors affecting the net section efficiency of a cold-formed steel channel brace bolted at the web by incorporating into the equation proposed in this paper for determining the net section tension capacity of a cold-formed steel channel brace bolted at the web.

Guven Kiymaz and Edip Seckin (2014) studied the behavior of steel tubular member welded end connections considering shear lag effect. Lip H. The *et al.* (2014) carried out a series of laboratory tensile test to reach the Net Section Tension Capacity of Equal Channel Braces Bolted at Different Legs. Based on a modification to the equation derived for channel braces bolted at one leg, a design equation is presented for determining the net section tension capacity of a cold-formed steel channel bracket bolted at different legs. Y. H. Xiong *et al.* (2015) studied the shear lag of high strength steel bolted and welded channels through finite element method. It was observed that the tensile capacity and final elongation of the HSS channels are considerably lower than those of the corresponding normal steel channels.

Abedin, Mohammad, *et al.* (2019a) studied shear lag effects in channels welded at both legs through considering connection eccentricity, connection length, gusset plate thickness, member-free length, and connection-free length in single- and double-channel sections welded at both legs. The results of the numerical analyses showed that, in single-channel connections, the effects of connection length, connection eccentricity, and gusset plate thickness are more pronounced, while in double-channel connections the last parameter is not very critical. They also propose novel approaches for fracture detection in steel girder bridges (Abedin *et al.* 2019b) using several method especially wireless sensor (Abedin *et al.* 2019b).

Current structural codes cover all modes of fracture in their design procedures. The present study concentrates on the net section rupture in which a coefficient called “shear lag coefficient” must be initially determined. To calculate this coefficient, structural code provisions propose several equations, all of which are based on the previous studies mainly conducted on riveted and bolted connections, and according to the recent parametrical investigations, applying such provisions can lead to a conservative design for welded connections. What is more, such equations do not consider the effect of symmetrical shape. Regarding the mentioned issues and the prevalent use of tensile connections with double channel sections, the effect of important factors like the connection length, the dimensions of section, the symmetry of section, and the member free length on shear lag coefficient will be evaluated by a parametrical analysis, after which the tensile performance of built-up box sections and double channel (front-to-front) sections will be compared. Shear lag coefficient (U) is defined as Eq.1.

$$U = P_u / F_u A_n \tag{1}$$

Where F_u is the ultimate strength of steel, A_n is net section area and P_u is the ultimate tensile load.

2. Material and methods

2.1 Provisions for designing members in tension

The AISC Specification for Structural Steel Buildings (AISC 360-16, 2016) proposes the following equations (Eqs.2-4) to be considered in designing members in tension:

1. Gross Section Tensile Fracture:

$$\varphi T_n = P_u / 0.9 A_g F_y \tag{2}$$

2. Net Section Tensile Fracture:

$$\varphi T_n = 0.75 A_e F_u \,.\, A_e = U A_n \,.\, U = 1 - \frac{\overline{x}}{l} \tag{3}$$

3. Shear:

$$\varphi T_n = min\{0.6 F_y A_g \,.\, 0.75 * 0.6 F_u A_{nv}\} \tag{4}$$

Where A_g is gross section area, A_n is net section area, A_{nt} is net area subject to tension, A_{nv} is net area subject to shear, A_g is gross area subject to shear, $\overline{x}$ is eccentricity of connection (the distance between the centroid of the section and the gusset) and l is connection length.

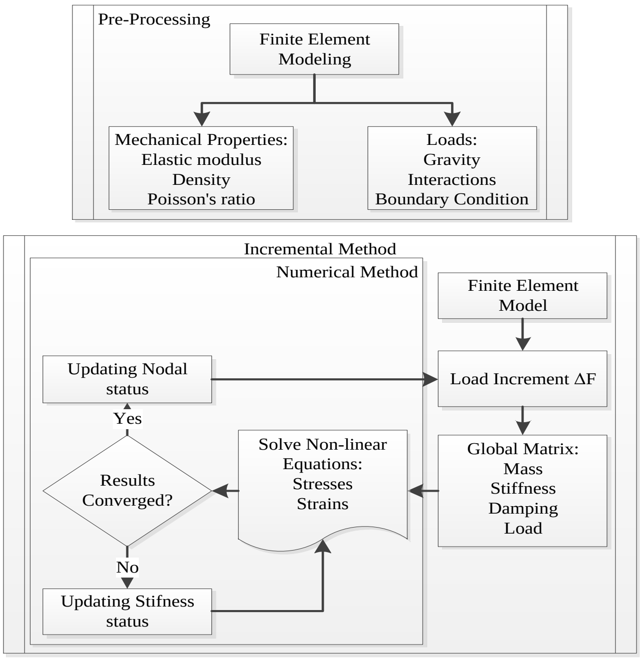

Fig. 1 general framework in numerical analysis

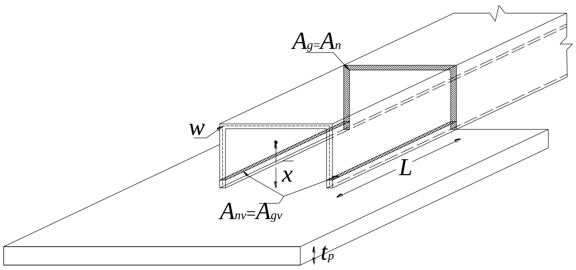

Fig. 2 Parameters of tensile design

3. Numerical analysis

3.1 Numerical modeling

The connection and structural elements are modelled by the means of ABAQUS 6.10 software and the general methodology in dealing with this numerical problem briefly illustrated in figure.1. With regard to the high plasticity of material and assuming a constant material volume in large deformations, the three-dimensional C3D8RH element, an 8-node hexagonal hybrid one with reduced integration, is used. The analysis is performed using the general static method whilst the effects of geometrical nonlinearity and the nonlinear behaviour of material are also taken into account. According to the symmetrical shape of the model along with the intention of minimizing the calculation costs, one-eighth and one-fourth of the connections are respectively modelled for double channels and single channels, and symmetrical support conditions are applied to symmetrical planes (Figure.2). Simulating a displacement-controlled loading, the gusset end is subjected to a gradual linear displacement. Since the purpose is only to examine the ultimate capacity of the tension member, it is supposed that the fracture occurs merely in the main member whereas the gusset plate and the weld would resist the subjected loading. This means that the deformations in the gusset plate and the weld would be far less than those of the tension member, hence an elastic behaviour can be presumed for the weld while an elastoplastic behaviour with isotropic hardening is used to simulate the tension member. The pivotal objective of the present paper is investigation of the parameters involved in the shear lag coefficient. Theoretically it is plausible to assume gusset plate and welds elastic and just observe the shear lag phenomenon as it is a separate phenomenon from gusset plate or weld fracture. In reality however the gusset plate or weld may fail prior to the channels but theoretically we can take the gusset and weld elastic and increase the load and observe the behaviour of the channel. It would not make the observations and the relationships between the parameters and shear lag coefficient absurd. The fracture simulation is performed using the ductile damage model provided in ABAQUS software. It is assumed that the fracture happens due to the growth, propagation and joining of the holes in material and besides, the strain at the beginning of fracture mechanism is considered as a function of stress triaxiality. Due to the importance of net section fracture in this study and considering the stress concentration in the connection region, an area with a 10-cm distance from the gusset edge is defined in which a finer mesh is chosen to acquire more reliable analysis results. The validity of results is then confirmed in accordance with the results of Hui Guo (2005) experimental studies.

Hui Guo investigated the tensile capacity of double channels with a back-to-back connection, the material properties of which are identically used in this study. ABAQUS modelling must be performed using true stress and true strain. Thus, the equations for converting engineering stress to true stress are used as follows (Eqs. 5-6):

$$\overline{\sigma} = \sigma(1+\varepsilon) \tag{5}$$

$$\overline{\varepsilon} = ln(1+\varepsilon) - \sigma/E \tag{6}$$

Where E is elastic modulus, σ is engineering stress, ε is engineering strain, $\overline{\sigma}$ is true stress and $\overline{\varepsilon}$ is true strain and figure. 3 illustrates the values of yield and ultimate stress as F_y is 360 MPa and F_u is 506 MPa.

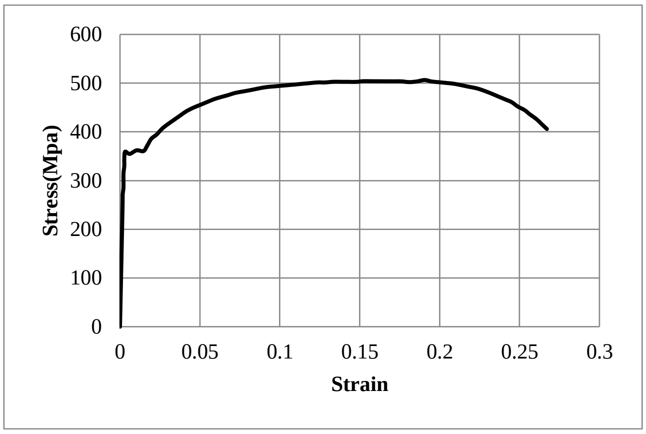

Fig. 3 Engineering stress-strain curve

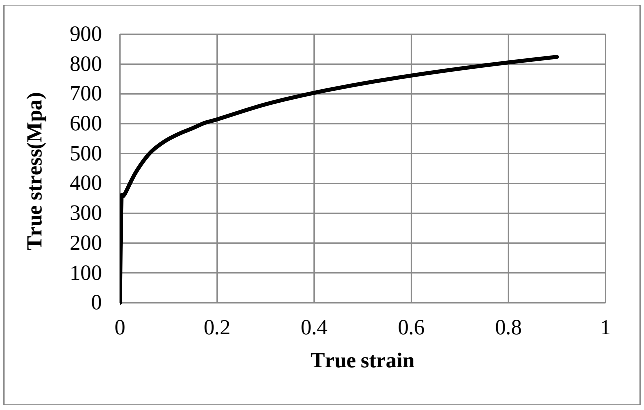

Fig. 4 True stress-strain curve

Converting equations can only be used to calculate the true stress before the necking stage, after which stress and strain would be concentrated on a particular point. On the other hand, the stress-strain curve must cover the range of strain up to 0.9 in order to depict the fracture. Hence, the below equation is proposed in Eq.7.

$$\sigma = K\varepsilon^{m} \tag{7}$$

Based on the diagram, the values of m and K are equal to 0.195 and 841.34 respectively. As these factors are obtained, the true stress-strain curve would be as figure 4.

The ductile damage model in ABAQUS software is used to simulate the fracture process. This model requires two input factors, the first one is the relationship between the fracture initiation strain and the stress triaxiality, and the other is the ultimate displacement, both of which will be further described. The relationship between the fracture initiation strain and the stress triaxiality is proposed as follows with reference to the study of Yu and Jeong (2010).

The ductile damage model with linear displacement damage evolution is employed in the finite element models to simulate the fracture process. As mentioned above the model requires two parameters, the ultimate displacement u_f and the fracture initiation strain $\bar{\varepsilon}_D^{pl}$. The threshold strain could be expressed by a function of stress thriaxiality η as:

$$\bar{\varepsilon}_D^{pl} = \begin{cases} \infty & \eta \le -1/3 \\ \dfrac{C_1}{1+3\eta} & -\dfrac{1}{3} \le \eta \le 0 \\ C_1 + (C_2 - C_1)(\eta/\eta_0)^2 & 0 \le \eta \le \eta_0 \\ \dfrac{C_2\eta_0}{\eta} & \eta \ge \eta_0 \end{cases} \tag{8}$$

$$\eta = {}^{\sigma_m}/_{\bar{\sigma}} \tag{9}$$

$$\sigma_m = \frac{1}{3}(\sigma_1 + \sigma_2 + \sigma_3) \tag{10}$$

$$\bar{\sigma} = \sqrt{\frac{1}{2}[(\sigma_1 - \sigma_2)^2 + (\sigma_1 - \sigma_3)^2 + (\sigma_2 - \sigma_3)^2]} \tag{11}$$

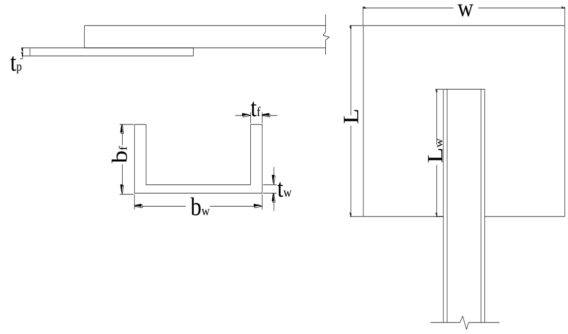

Fig. 5 Dimensions of members in finite element analysis

In this equation (Eq. 8), η represents the coefficient of triaxial stress and the value of C_2, being normally equal to 0.8 for structural steel, could be obtained from the tensile test of standard specimen by using Eqs. 9-13.

$$C_2 = -\ln(1 - A_R) \tag{12}$$

A_R Stands for the percent reduction of area and the coefficient of C_1 can be calculated by the below equation in which the factor of m is equal to that of Eq. (7).

$$C_1 = C_2\left(\frac{\sqrt{3}}{2}\right)^{1/m} \tag{13}$$

The parameter m is the stress-strain hardening relation and is evaluated as 0.195. Besides these, in accordance with the reference Yu and Jeong, η_0 is fixed to 1/3. There remains two free parameters C_2 and u_f which are determined with try and error method. Several models of a tensile coupon test are built and run and the resultant stress-strain relation is compared to the experimental stress-strain curve derived from the Hui Guo work. The parameters that best match the experiment are determined as $C_2 = 0.8$ and $u_f = 0.005m$.

The general static analysis is used in the model. The material would be degraded complying with the damage evolution path defined for the model and as the damage index D for any element equals 1 the element stiffness would be zero however it is not eliminated visually. figures. 6-8 show an acceptable conformity for the numerical model and the experimental results from Hui Guo study.

3.1 Model validation

Three different models are developed by the ABAQUS 6.13 software to assess whether the properties of materials, being assumed in accordance with the experimental studies of Hui Guo (2005) are valid. The C75×6 channel is used in all models as it is shown in figure 5 alongside the dimensions of the gusset plate. The channel sections are connected to the gusset in a back-to-back form (The web of channel section is in touch with the gusset plate) and a single channel section is used for one of the models. Referring to the study of Hui Guo, a value of 1 is supposed for the plastic strain at the fracture moment. Identifying the fracture stage is only possible by an evaluation on the stress

Table 1 Gusset and channel dimensions

Gusset/ channel	w	L	t_p (mm)	t_w (mm)	b_w (mm)	b_f (mm)	t_f (mm)
Gusset1	300	370	12.7	-	-	-	-
Gusset2	300	480	12.7	-	-	-	-
Channel	-	-	-	4.3	76	35	6.9

* in all the above specimens the free length of the members is 1200 mm.

Table 2 Comparison of Analytical and Experimental Results

Gusset type	$Pu_{FEM}(kN)$	$Pu_{test}(kN)$	FEM failure mode	Test failure mode	Weld Length (mm)	Weld Size (mm)	Single/Double	Model
2	761	752	GF	GF	115	5	Double	1
1	381	366	GF	GF	100	5	Single	8
2	761	741	GF	GF	100	5	Double	9

* GF=Gross section fracture

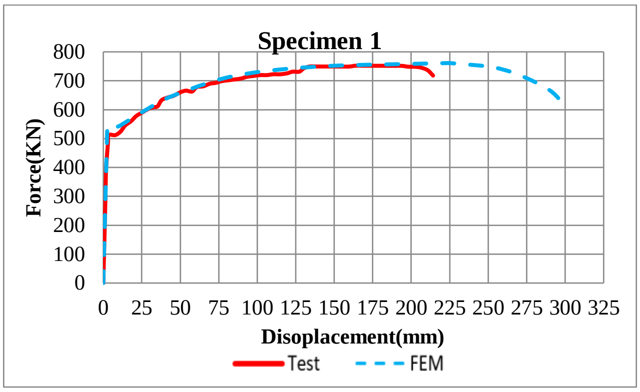

Fig. 6 Comparison of Analytical and Experimental Tensile Behavior of specimen 1

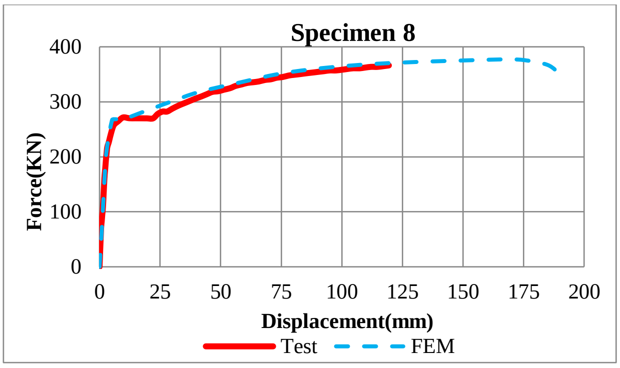

Fig. 7 Comparison of Analytical and Experimental Stress-Strain Curve of specimen 8

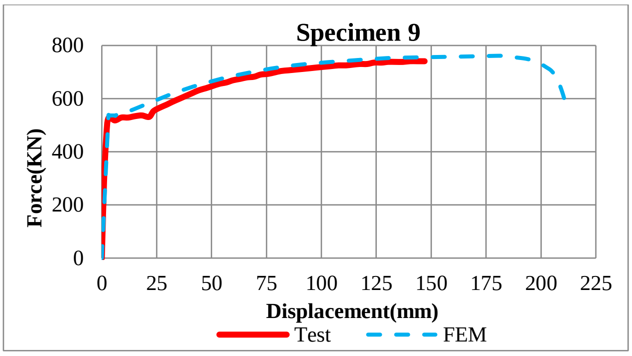

Fig. 8 Comparison of Analytical and Experimental Tensile Behavior of specimen 9

level. Prior to the fracture stage, there would be a rise in the stress value and as the strain increases, the fracture stage begins, after which the stress value gradually decreases. The cracking stage is usually initiated with a plastic strain reaching around 0.8 to 1.0 and such strain values can be seen in a vast region of adjacent elements. Afterwards, large deformations would occur in different elements and as such, the model would lose its reliability. So, numerical models can only be used before the beginning of the fracture stage. Gusset plate and channel section dimensions are illustrated in Table 1 and the details of each model alongside the analyses results are presented in the Table 2. The failure modes in samples 1, 8 and 9 are also shown in figures 9-11.

4. Numerical results and discussion

4.1 Identifying the fracture mode from analyses result

A tension member is liable to fail in various modes and the section of the member should be designed to prevent failure by any of these modes.

4.1.1 Gross Section Fracture

This mode of fracture occurs in the gross section of tension member, with a distance from the connection (figure 12). This state can be distinguished when a necking stage as well as high strain is observed in the middle of the member. Since the fracture takes place in an extensive area, the analysis will fail to cover the complete fracture and it cannot proceed to the necking stage while becoming so slow due to the numerical issues. Thus, gross section fracture can be identified in case the tensile load in the member is almost equal to the load capacity of the member and the plastic strain is measured to be around 0.2.

4.1.2 Net Section Fracture

The net section rupture strength of a member is based on

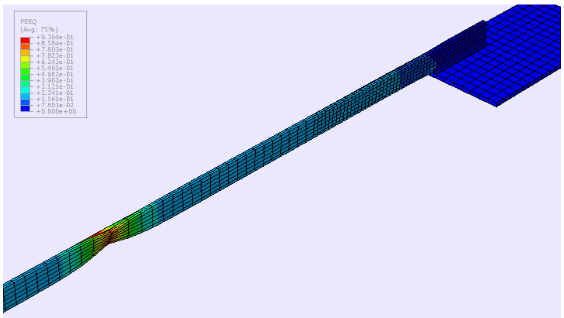

Fig. 9 The Fracture of Specimen 1

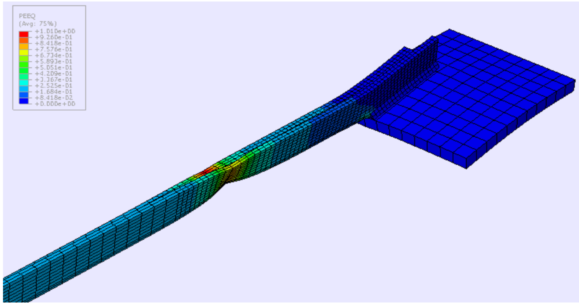

Fig. 10 The Fracture of Specimen 8

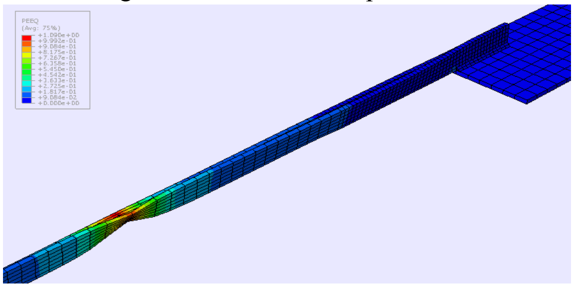

Fig. 11 The Fracture of Specimen 9

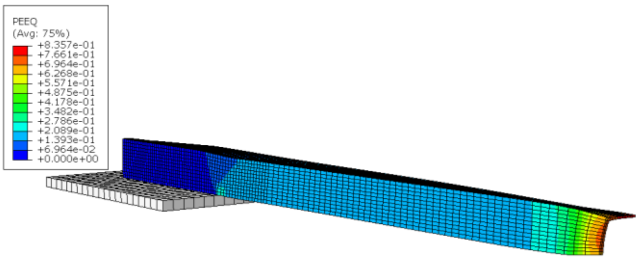

Fig. 12 Gross Section Fracture in Numerical Model

the fracture of the net area of the cross-section. With this fracture mode high level of stress concentration is observed in the start of the weld adjacent to member to gusset connection and the rupture begins as the plastic strain reaches around 0.8. Large deformations develop and propagates around the circumference of the tension member as is shown in figure 13.

4.1.3 Shear rupture

Shear rupture can be recognized by witnessing stress and strain concentration along the connection length. At the first steps of loading, stress and strain concentration occurs at the start and end of the weld.

As the shear rupture failure mode occurs, high level of stress and strain concentration is observed along the welds especially at the ends of the weld length and by increasing the tensile load, rupture begins from the start of the connection length which is observed as high level of equivalent plastic strain around 0.8. Large shear deformation would build up along the weld which is well distinguishable (figure 14).

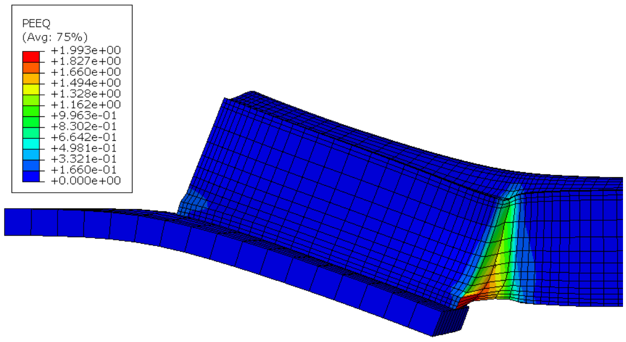

Fig. 13 Net Section Fracture in Numerical Model

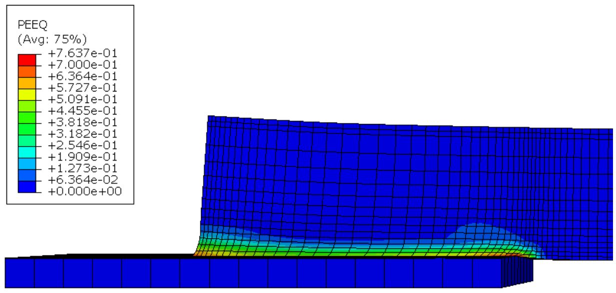

Fig. 14 Shear rupture in Numerical Model

4.2 Specification of used channels

The analyses in this study are carried out for the connections of single and double channels including C12, C14, C16 and C18 sections. The impact of various factors such as the weld length (L), the eccentricity of axial load ($\bar{x}$) and the circumference of the section (w) are investigated in these cases. Also, other factors like the gusset thickness (tp) and the gusset free length (a) are studied for the single-channel connection owing to the bending of the gusset plate. Relevant parameters and dimensions in channel sections are shown in figures 15-16 and Table 3 respectively.

Different numerical models are named in accordance with their properties being respectively presented in the appendixes tables. For instance, “C16-17-d-S” describes the model with a C16 section type, a connection length of 17 cm, double channels while the member free length is considered as short or equal to 80 cm.

4.3 Analyses results of single channels

4.3.1 The gusset free length (a)

Regarding the possibility of bending moment development in the gusset plate due to its freedom of movement, the stress concentration in the fillet weld leg near the gusset edge will result in a net section fracture. The more eccentric is the load, the more intense would be the

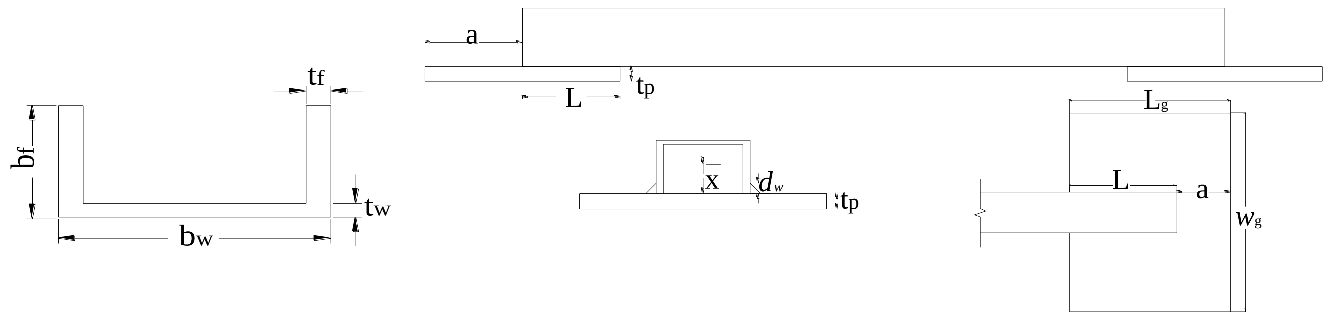

a) Section details b) single channel details

Fig. 15 Parameters of analysis in section and single channel section

stress concentration as well as the bending moment. If supposed that all other factors are constant, increasing the free length of the gusset would lessen the required bending stress in the outer fibers of the section in order to bend the gusset and therefore, the tensile capacity would increase. Weld lengths of 12 and 15 cm, respective gusset width and thickness of 30 and 1.5 cm, a fillet weld size of 8 mm and a member length of 1.2 m are considered for all different sections so as to study the effect of the gusset free length, being equal to distinct values of 5, 10 and 15 cm.

As the tensile load in the member increases during the loading process, so does the moment of eccentricity which is equal to F.d (Figure 15a). This moment disturbs the uniform stress distribution over the cross section in way that the upper fibers would be subjected to a lower stress level. Such non-uniform stress distribution alongside the shear lag effect arising from the non-uniform load transfer from the channel to the gusset plate causes stress concentration in the connection region. On the other hand, the gusset plate bends under the imposed moment of F.d, and this will raise the stress concentration. The direction of mentioned bending leads to a reduction in the moment arm (d), hence in the imposed moment. So, it can be concluded that the gusset plate bends more easily under a lower tensile load when the gusset free length (a) is increased, and because the impacts of the imposed moment and the shear lag are reduced, the tensile capacity would be enhanced.

Decreasing the gusset thickness while other factors are constant develops more bending moment at the end of the weld and it increases the stress concentration in the critical section. Although the tensile capacity would be reduced, the efficiency of the section would not be significantly influenced.

Figures 17 to 20 depict the tensile capacity of the single channel with a C12 section type and a weld length of 12 cm whereas the gusset width is equal to 30 cm and the gusset thickness and free length are each divided into 3 different values.

This length is found as the most important factor in the shear lag coefficient of a tension member. Increasing the weld length reduce the stress concentration at the start and end of the weld and the tensile capacity would be enhanced. The results of studying this factors are illustrated in Figure 17.

4.3.2 The gusset thickness (t_p)

According to Figure 18, as expected, the thickness of the gusset has little effect on the tensile capacity, but as the thickness of the gusset increases, the tensile behavior improves slightly, but this effect decreases with increasing connection length.

Table 3 Dimensions of sections

Area-model (mm^2)	Area-STAHL (mm^2)	t_f (mm)	t_w (mm)	b_w (mm)	b_f (mm)	Section
1480	1540	8	5	120	60	C12
1780	1840	9	5	140	65	C14
2105.5	2170	9.5	5.5	160	64.5	C16
2460	2510	10.5	5.5	180	775	C18

* Stahl Im Hochbau

4.3.3 The member free length

Apart from the aforementioned models, other models are developed to examine the effect of the member free length on the tensile capacity. As it is shown in Figures 19 and 20. This factor is not that influential and can be neglected.

4.3.4 The Effect of connection length

As the connection length is increased in the case of double channels, transmitted through the weld to the gusset, this phenomenon reduces the stress through distributing over a longer period, resulting in a more uniform distribution of force. The shear lag caused by the uneven distribution of force at the connection is attenuated and the shear lag coefficient and tensile capacity of the connection increase, in addition to the high impacts on single channels, another important phenomenon occurs with increasing connection length. Which contributes greatly to increasing the tensile capacity of the member.

To explain this effect, consider two single channels with equal conditions except length of connection, as shown in figure 21, with equal tensile force, equal moment will be induced at both gussets and two gussets are bent at equal interval a, but in the case of channels with longer connection length, this bending reduces the amount of eccentricity, which reduces the effects of centrifugal moment and the shear lag. Therefore, tensile capacity increases to some extent.

As shown in figure 21, the following conditions would occur under the equal forces of F and with equal lengths a.

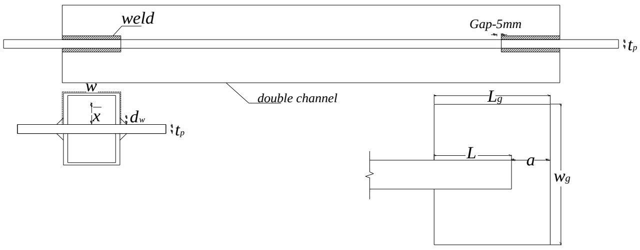

a) double channel details

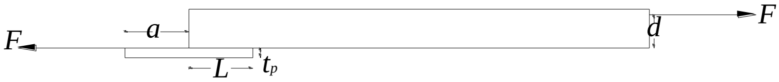

b) The eccentricity of axial load

Fig. 16 Parameters of analysis in eccentricity loading and double channel section

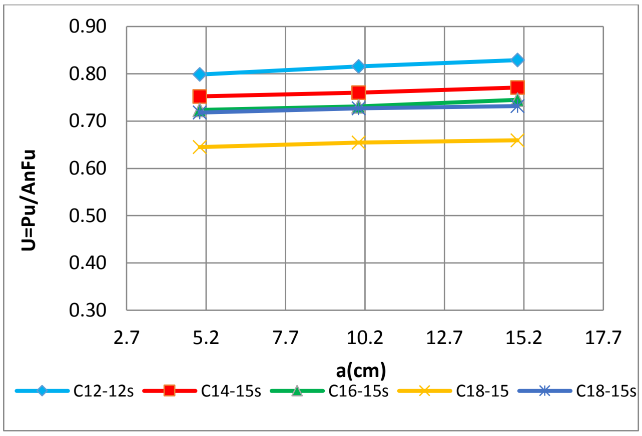

Fig. 17 The effect of gusset free length on single channel tensile efficiency

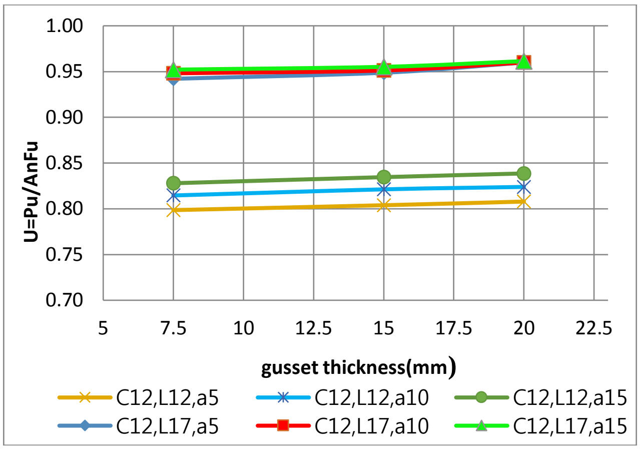

Fig. 18 The effect of the gusset free length on the tensile capacity of single channels

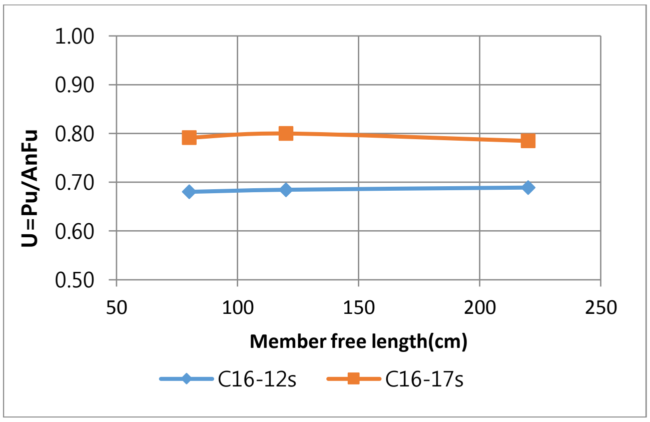

Fig. 19 The effect of member free length on the tensile capacity of single channels

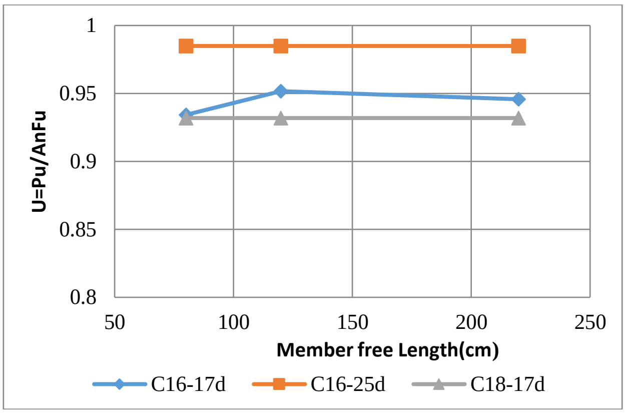

Fig. 20. The Effect of Member Free Length on the Tensile Capacity of Double Channels

$$L_2 > L_1 \quad \rightarrow \quad h_2 > h_1$$

As shown in the Figure 22, increasing the connection length greatly increases the breakdown capacity of the cross sections. Another interesting point is that in models with a joint length of 17 cm compared to models with a joint length of 12 cm, the increase in the distance between the end of the Channel and the end of the gusset (a), has a much smaller effect on the final load of the member, because in the cases with longer connections, gusset has more freedom to move and therefore decreases the load eccentricity, so increasing the length 'a', does not greatly improve this advantage.

4.3.5 The eccentricity of axial load ($\bar{x}$)

When the eccentricity of axial load is increased, the force must be transferred to the gusset plate via a longer

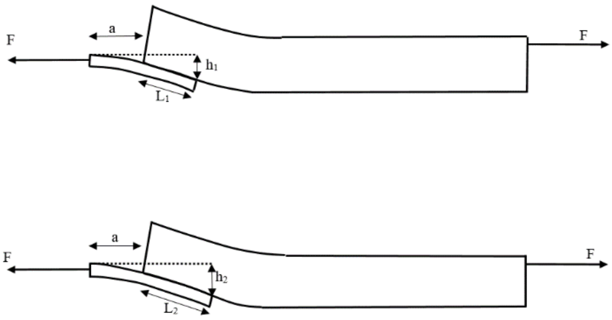

Fig. 21. Schematic representation of welding length effect

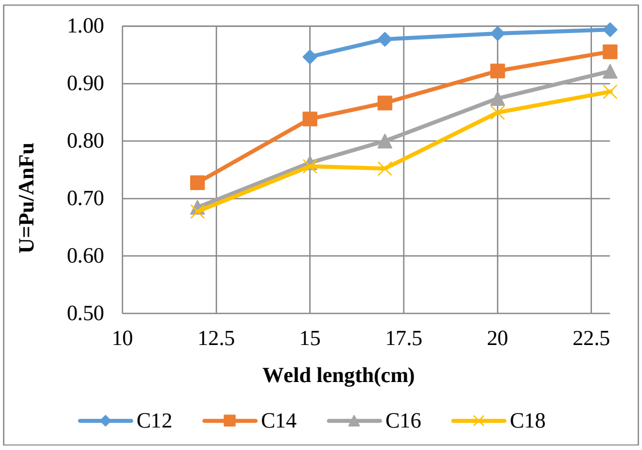

Fig. 22 Effect of weld length on tensile capacity of single Channels

path that raise the effect of the shear lag. The parametric investigation of the weld length and the eccentricity of axial load is carried out by considering the gusset plate with a width of 30 cm, a thickness of 1.5 cm and a free length of 10 cm while the fillet weld size and the member free length are supposed equal to 8 mm and 1.2 m, respectively. Five separate values for the weld lengths are also considered as 12, 15, 17, 20 and 25 cm.

Finally, the ratio of $\frac{\bar{x}}{L}$ versus the shear lag coefficient is demonstrated in Figure 23 and the results are then compared with the estimates of the AISC-LRFD. Different fracture modes are referred by their abbreviations and their region of dominance is bounded by vertical lines. Besides, the shear lag coefficient of the section is determined by using the Eq. (1). Other structural codes such as the design code of Canadian Standard Association (CSA, 2014) use the ratio of L/w rather than $\frac{\bar{x}}{L}$ (The parameter w is circumference of the channel section). Thus, the ratio of tensile efficiency derived from the numerical analyses is compared to the shear lag effect proposed by the CSA code, and the diagrams are shown in Figure 24 (NF stands for Net Section Fracture).

As it can be seen in figure 23, the AISC code is accurate enough whilst the equations provided in the CSA code are about 25% more conservative and the resulted coefficient has a wide disparity with the analytical value. An alternative equation can be proposed as Eq. 14.

$$\begin{cases} U = 0.4 + \dfrac{0.618l}{w} & \dfrac{L}{w} \leq 0.97 \\ U = 1 & l/w > 0.97 \end{cases} \tag{14}$$

These equations are derived by fitting the best linear curve to the data in the case of net section fracture. R^2 values are presented. Equation 14 obtained with R^2=0.89.

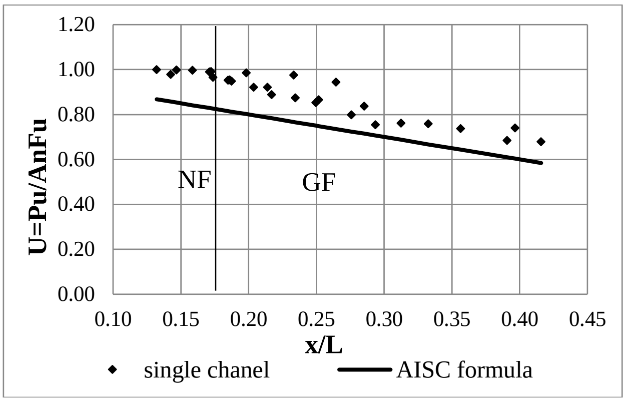

Fig. 23 Comparison of the Analytical Tensile Capacity and the proposed equation of AISC

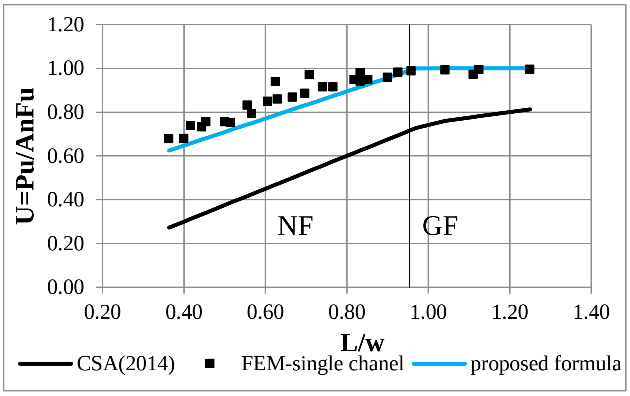

Fig. 24 Comparison of Analyses Results, the estimate of CSA-2014 and the proposed equation for double channels

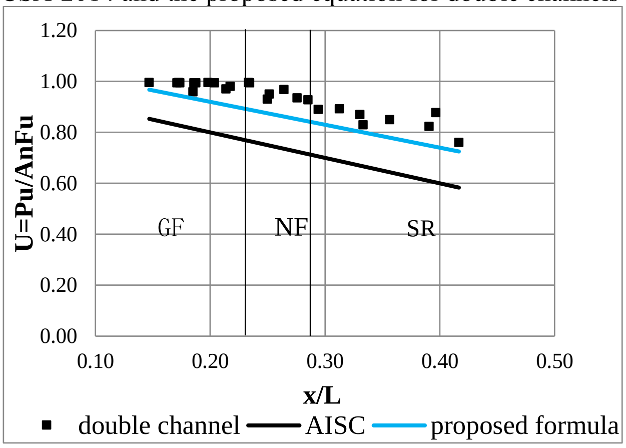

NF:Net section Fracture,SR:Shear Rupture, GF:Gross section Fracture

Fig. 25 Comparison of the Tensile Capacities derived from the AISC and the proposed equation

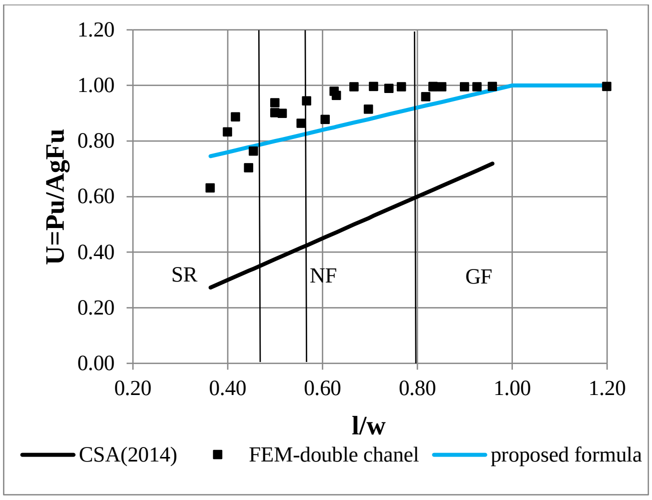

Fig. 26 Comparison of the CSA estimate and the proposed equation for double channels

4.4 Analyses results of double channels

The double channel section with a front-to-front connection form are investigated under the changes in factors like the eccentricity of axial load and the weld length. Regarding the symmetrical shape of double channels, the gusset plate does not bend and its thickness, therefore, has no effect on the ultimate tensile capacity of the section. That is why the gusset thickness is neglected in this part of parametric investigation. Once again, the weld length and the eccentricity of axial load are the first and second key factors affecting the tensile capacity. All the assumptions with regard to the parametric investigation of these factors in single-channel connections are similarly made for double channels. Figure 26 demonstrates the shear lag coefficient (U) versus the ratio of $\frac{\bar{x}}{L}$ while the value of $\bar{x}$ is considered equal to that of the double-channel section. The regions of dominance of each fracture mode are bounded by vertical lines.

Comparing the diagrams in Figure 23 and 25, it can be stated that the shear lag effect of double channel sections is roughly 10% larger than its counterpart for single-channel sections. The results of the finite element analyses are eventually compared to the proposed equations of CSA. Figure 25 shows how the shear lag coefficient obtained from the CSA provisions is extremely conservative and has a disparity of approximately 35% with the analytical value. The following equations (Eqs. 15-16) are proposed to calculate the shear lag coefficients for double channel sections:

- Based on the ASIC-LRFD:

$$\begin{cases} U = 1 \quad . \quad \dfrac{\bar{x}}{L} < 0.11 \\ U = 1.1 - \dfrac{0.9\bar{x}}{L} \; . \; \dfrac{\bar{x}}{L} \geq 0.11 \end{cases} \tag{15}$$

Equation 11 obtained with R^2=0.89.

- Based on the CSA (2014):

$$\begin{cases} U = 1 \, . \quad \dfrac{L}{w} > 1 \\ U = 0.6 + \dfrac{0.4L}{w} . \; \dfrac{L}{w} \leq 1 \end{cases} \tag{16}$$

Equation 11 obtained with R^2=0.24

5. Conclusions

A numerical simulation procedure for parametric Investigation of shear lag effect on fillet-welded connections of tension members consisting of single or double channel sections has been proposed in this study.

- It can be concluded from the results that the proposed equation by AISC code (AISC [7]) is reliable to determine the shear lag coefficient for single-channel sections whereas it is quite conservative to be used for double channel sections. To step toward a more economical design of tension members, alternative equations are proposed. A summary of this research is presented in Table 4.
- Furthermore, the tensile behavior of single and double channel sections are compared to each other. Due to its symmetrical shape, a double channel section has a larger shear lag coefficient and is subjected to less stress concentration in comparison with a single channel section having the same ratio of $\frac{\bar{x}}{L}$. To make sure about the analyses and results, more experimental studies must be conducted, and in order to propose a more general equation considering the effect of section symmetry on calculating the shear lag coefficient, similar researches must be carried out on other common symmetrical sections.
- The study revealed that the gusset thickness and the member length are not influential in the determination of the tensile capacity as well as the shear lag coefficient of symmetrical double-channel section; however, they slightly affect the tensile capacity of single-channel sections owing to their symmetrical shape. For example, as a result of decreasing the thickness of the gusset plate, it would bend more easily and creates stress concentration in outer fibers of the member that reduces the tensile capacity. Also, the gusset plate would have more freedom to bend when its free length is increased. This is the reason why there would be a drop in the shear lag effect and the tensile capacity would be enhanced. Moreover, the fillet weld size has no significant effect on the shear lag coefficient whilst the most important factors are the weld length and its ratio to the section dimensions (including the eccentricity of axial load).
- Considering the fact that equations proposed by structural codes are based on the previous studies conducted on riveted and bolted connections, using them can lead to a conservative and uneconomical design for welded connections. This study revealed that the AISC code is reliable in calculating the shear lag coefficient of single channel sections whilst the equations provided in the CSA code result in a coefficient being about 30% less than the analytical one. For double channel section, the equations of

the AISC and the CSA are more conservative by 20% and 40%, respectively.

- The symmetrical shape of sections is not considered in the current structural codes whereas increasing the eccentricity of axial load lead to a growth not only in the shear lag effect, but also in the imposed moment. More often than not, this bending moment has more effects on the tensile capacity than the shear lag. Therefore, a symmetrical section can prevent the development of such a bending moment and reduces the stress concentration in the critical section that improves the performance of tension members. To be more precise, the shear lag coefficient for single channel sections is generally about 10% less than that of double channels and neglecting this fact will undoubtedly result in a non-optimal design. The alternative equations to determine this coefficient are proposed as in equations 14 and 16. Also, the coefficient derived from these equation is more than the estimates of the AISC and the CSA by the respective percentages of 10% and 40%.

Acknowledgments

This researches received no external funding.

References

ABAQUS (2013), Analysis User's Manual. Version 6., Dassault Systemes Simulia, Inc.

Abedin, Mohammad, Shervin Maleki, Nafiseh Kiani and Esmail Shahrokhinasab, (2019), "Shear Lag Effects in Channels Welded at Both Legs", *Adv. Civil Eng.*. **2019**, Article ID 8041767, 10. https://doi.org/10.1155/2019/8041767

Abedin, Mohammad, and Armin B. Mehrabi. (2019), "Novel approaches for fracture detection in steel girder bridges", *Infrastructures*, **4**(3), 42-59. https://doi.org/10.3390/infrastructures4030042.

Abedin, M., S. Farhangdoust, and A. B. Mehrabi. (2019), "Fracture detection in steel girder bridges using self-powered wireless sensors." *Proceedings of the In Risk-Based Bridge Engineering: Proceedings of the 10th New York City Bridge Conference*, NY, U.S.A, August.

AISC, (2016), "Specifications for structural steel buildings", *ANSI/-AISC360-16*, Chicago.

ASTM A370, (2001), "standard test methods and definitions for mechanical testing of steel product", *American Society for Testing and Materials*, https://doi.org/10.1520/A0370-19E01

Benaddi D. and Bauer D. (2003), "Finite element analysis of double channel truss connections", *Proceedings of the General Conference, 31st Annual Conference of the CSCE*, Moncton, Canada, May.

CSA (2014), "S16-14 Limit States Design of Steel Structures", *Canadian Standard Association*, Toronto, Canada, https://doi.org/10.1061/(ASCE)0733-9445(1984)110:2(275)

Easterling and Gonzalez Giroux (1993), "Shear Lag Effects in Steel Tension Members", *Eng. J.*, American Institute of Steel Construction, U.S.A.

Easterling W.S. and Gonzales L. (1993), "Shear Lag Effects in Steel Tension Members", *AISC J. Eng.*, **30**(2), 77-89.

Gaylord E.H.Jr, Gaylord C.N., and Stallmeyer J.E. (1992), *Design of Steel Structures, 3rd Edition*, McGrow Hill, NY, U.S.A.

Guo, H. (2005), *Shear Lag Effects on Welded Hot-rolled Steel Channels in Tension*, University of Alberta, Edmonton, Canada.

Guven Kiymaz and Edip Seckin (2014), "Behavior and design of stainless steel tubular member welded end connections", *Steel Compos. Struct.*, **17**(3), 253-269, https://doi.org/10.12989/scs.2014.17.3.253

Humphries Matthew J.R. and Birkemoe Peter C. (2004), "Shear lag effects in fillet-welded tension connection of channels and similar shapes", *Connections Steel Struct.*, **5**(1), 114-121.

L. H. Teh and B. P. Gilbert (2013), "Net section tension capacity of cold-reduced sheet steel channel braces bolted at the web," *J. Struct. Eng.*, **139**(5), 740–747. https://doi.org/10.1061/(ASCE)ST.1943-541X.0000650

L. H. Teh and B. P. Gilbert (2014), "Net section tension capacity of equal channel braces bolted at different legs," *J. Struct. Eng.*, **140**(6), Article ID 06014002, https://doi.org/10.1061/(ASCE)ST.1943-541X.0000964

L. H. Teh and V. Yazici (2013), "Shear lag and eccentricity effects of bolted connections in cold-formed steel sections," *Engineering Structures*, **52**, 536–544. https://doi.org/10.1016/j.engstruct.2013.03.024

Luigino Dezi, Fabrizio Gara and Graziano Leoni (2003), "Shear-lag effect in twin-girder composite decks", *Steel Compos. Struct.*, **3**(2), 111-122, https://doi.org/10.12989/scs.2003.3.2.111

Munse W.H. and Chesson J.R. (1963), "Riveted and Bolted Joints: Net Section Design", *J. Struct. Division*, **89**(5), 475-482.

Orbison J.G., Wagner M.E., and Fritz W.P. (1999), "Tension plane behavior in single-row bolted connections subject to block shear", *J. Construct. Steel Res.*, **49**(3), 225-239, https://doi.org/10.1016/S0143-974X(98)90172-9

Wang Q.F. (1997), "Lateral buckling of thin-walled members with openings considering shear lag", *Struct. Eng. Mech.*, **5**(4), 369-383, https://doi.org/10.12989/sem.1997.5.4.369

Won-Sup Hwang, Young-Pil Kim, and Yong-Myung Park (2004), "Evaluation of shear lag parameters for beam-to-column connections in steel piers", *Struct. Eng. Mech.*, **17**(5), 691-706, https://doi.org/10.12989/sem.2004.17.5.691

Y. H. Xiong, A. C. C. Lam, M. C. H. Yam, and K. F. Chung (2015), "Numerical study of shear lag of high strength steel bolted and welded channels," *Congress of Advances in Structural Engineering and. Mechanics*, Incheon, August.

Yu H.L. and Jeong D.Y. (2010), "Application of a stress triaxiality dependent fracture criterion in the finite element analysis of unnotched charpy specimens", *Theoretical Appl. Fracture Mech.*, **54**(1), 54-62, https://doi.org/10.1016/j.tafmec.2010.06.015

CC